GANIT

GANIT: Journal of Bangladesh Mathematical Society

**GANIT***J. Bangladesh Math. Soc.* 46.3 (2026) 068–081
DOI: https://doi.org/10.3329/ganit.v46i01.89343

# Investigation of Thermomagnetic Convective Flow in a Vertical Layer of Ethylene Glycol Based Magnetic Fluid Under the Effect of Inclined Magnetic Field

Md. Habibur Rahman[a*] and Sushmita Mondal[a]

[a] Department of Mathematics, Khulna University of Engineering & Technology, Khulna 9203, Bangladesh

## ABSTRACT

The linear stability of thermomagnetic convection in the ethylene glycol based magnetic fluid layer enclosed by two differentially heated walls. Ethylene glycol ($C_2H_6O_2$) is a colourless and sweet tasting viscous liquid. The goal of this article is to examine the impacts of thermo-gravitational buoyancy and magnetic forces due to the effects of orientation angle and intensity of magnetic field. The pseudo-spectral Chebyshev expansion technique is employed using Matlab software to produce the suitable numerical results. The intensity and inclination angle of the applied magnetic field play a critical role in stabilization in the flow domain. The destabilizing magnetic field variation effect is most pronounced in close to walls, particularly near the cold wall. However, viscous dissipation near the cold wall is likewise greater than that near the hot wall. As a result, the general instability pattern moves to the hot wall. Gravitational buoyancy due to thermal effects drives the instability more than magnetic effects. The magnetic fluids that are less sensitive to thermomagnetic changes than their more sensitive counterparts exhibit greater stability in the flow domain. With disregard for the linear magnetization rule, the differences in the critical values of the wave number, wave speed, and magnetic Grashof number are more pronounced for field orientation angles between $0^o$ and $90^o$. However, the results reveal that variations in Prandtl number, Pr significantly influence the growth rate and stability characteristics of the flow. The higher Prandtl numbers Pr tend to enhance the stabilizing effects of the magnetic field, delaying the onset of instability, whereas lower values promote thermal diffusion and shift the instability thresholds accordingly. This comparative analysis elucidates the critical role of thermal transport properties in conjunction with magnetic and buoyant forces, offering valuable insight into the underlying physical mechanisms governing MHD boundary layer stability.


**Received:** November 09, 2025 **Accepted:** March 14, 2026 **Published Online:** June 15, 2026
**Keywords:** Magnetic fluid; Convection; Magnetic field; Prandtl number; Stability.

*Corresponding author: hrahman180@math.kuet.ac.bd

## 1. Introduction

Magnetism is an inherent property exhibited by certain transition metals like cobalt, iron, nickel etc. and their alloys and mineral composites containing these elements. The magnetic characteristics of these materials progressively weaken with increasing temperature and eventually vanish at a specific temperature known as the Curie point, beyond which the material loses its spontaneous magnetization. A typical ferrofluids are made up to 10% of very thin magnetic particles, 10% of surfactant and 80% carrier liquid by volume [1].

This means that even under extremely intense magnetic fields, the material particles do not make aggregation or phase split. This indicates that, even under very strong magnetic fields, the solid elements in the suspension remain stable, showing neither agglomeration nor phase separation. Although studies on the properties of such magnetic colloids began in the 1930s [2], research efforts expanded markedly during the 1960 and 1970 decades, when industrial-scale manufacturing with magnetic fluids turn on adequately [3]. Nowadays the existence of large amount of literature about the properties of ferrofluids are available, for example, [4, 5, 3, 6, 7] and references therein. The fluids have no net magnetization when magnetic field removed, hence the magnetic moments placed in an alternating magnetic field releases heat. The ferrofluids obey the Curie's law as they are paramagnetic, and thus become less magnetized at higher temperatures. Such temperature sensitive ferrofluids induce especially strong practical interest [8]. In natural convection, fluid motion is driven by buoyancy forces arising from temperature differences. Conversely, in the case of advection that is in forced convection, the fluid is set into motion by external mechanical means such as pumps or fans. Artificial magnetic fluids, commonly known as ferrofluids, can be strongly magnetized when subjected to an external magnetic field, and then fluid is compiled with nano-particles of magnet up to 100 times miniature in size compared to the wavelength of visible light. For example; magnetite ($Fe_3O_4$) and hematite ($Fe_2O_3$) are most commonly used as stronger magnetic colloidal in the branches of magnetic fluids. Each and every fluid nano-particle is overlaid with a proper surfactant and the resultant fluid is called as surfacted ferrofluid shown in Fig. 1.1.

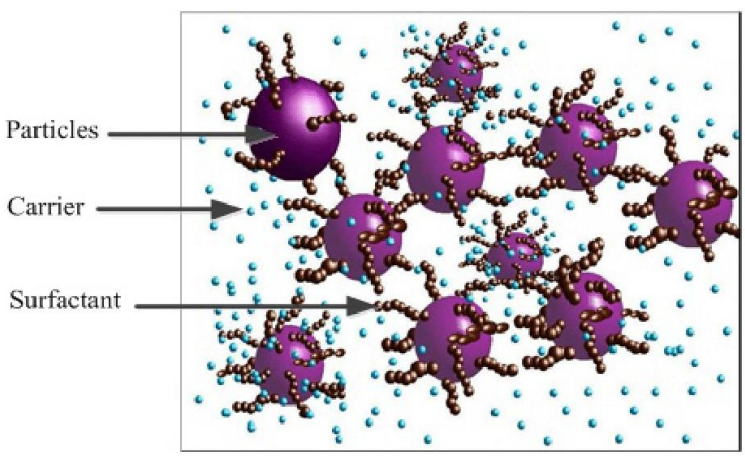


Fig. 1.1. Surfacted ferrofluid [9] utilized by permission.

When a magnetic field is employed into a ferrofluid then the fluids nano-particles are enticed and as a result the ferrofluid will experience a Kelvin body force, inducing a fluid flow along the thermal gradient. The ferrofluid can be driven by this thermomagnetic convection without a pump. The microfluidic systems have employed a choice of works where magnetic fluids are submitted in this review. Some of the convenience of magnetic manipulation compared to transfer properties as well as not being forced by pH and electric manipulation contain the ability to control both flow, surface charges or ionic intentness. Moreover, the nanoscopic properties of ferrofluids are not yet fully realize and must be further studied to really exploit their identical properties. Ferrofluids are thoroughly appointed in art and many branches of engineering field. In the branch of medicine for detection the cancer, ferrofluids can be conducted as a contrast agents for generating the magnetic resonance imaging. This article will analyse the characteristics of thermomagnetic convection in the ethylene glycol-based magnetic fluid layer. Ethylene glycol is a viscous liquid, colourless, sweet-tasting, whose chemical formula is ($C_2H_6O_2$). The major uses of ethylene glycol as an antifreeze agent

in coolants. The Prandtl number of ethylene glycol varies with temperature but generally falls between 5 and 150 for water-ethylene glycol mixtures, and its Prandtl number is arbitrarily chosen as 40.36 at room temperature for numerical results of this research, reported in [10]. The uniform hotness source and magnetic field are considered for this study. Over the last few decades, the application of magnetic and electric fields in fluid flow control achieved a considerable observation with prospects in the region such as designing, solid particles. The instability patterns have been recognized when the applied field is prototypical to the plates spreading thermomagnetic or thermo-gravitational waves and comprise of stationary magneto convection rolls [11]. The multiple-relaxation-time (MRT) lattice Boltzmann method (LBM) with GPU acceleration has been used to numerically integrate the natural or free convection flow in an open cavity filled with ethylene glycol-$AL_2O_3$ nanofluid reported in [12]. Numerical simulations with different controlling parameters have been carried out for a fixed Prandtl number Pr=16.6. The volume percentage and Rayleigh number of nanofluids are found to increase the magnitude of the locally dispersed Nusselt number. The effects of temperature-dependent viscosity on the natural convection flow from a vertical permeable circular cone with homogeneous heat flux are examined by Farhad et al. [13]. It is observed that, for small Prandtl numbers (Pr), the viscosity is a linear function of temperature. The local maxima of viscosity is greatly raised by a large perturbation solution, especially at low Pr, whereas the effect on the temperature distribution is less significant in the same conditions. In a vertical layer of ferrouid surrounded by two differently heated walls, the linear stability properties and energy distribution resulting from the combined effects of thermal, magnetic, and gravity forces are analysed in [14]. The pseudo-spectral Chebyshev collocation expansion approach is used to generate the numerical findings. It is discovered that, in contrast to magnetic effects, gravitational buoyancy is primarily responsible for the instability owing to thermal effects. Viscosity dissipation and modification of the applied magnetic field in the flow domain cause the perturbed kinetic energy to be lost. For the current study, it will be investigated a 3-D geometry with a tall vertical and wide fluid layer kept in a uniform magnetic field applied obliquely. The one side of the layer is cold by a cooler, and its other side is heated with a thermal field. The manual way of their most prominent features will likewise and the so-induced instability characters be analysed in the ethylene glycol-based magnetic fluid layer to initiate the comparative directions to the future applications for industrial productions.

## 2. Model Formulation and Mathematical Representation of Governing Equations

As depicted in Fig. 2.1, the system consists of a ferromagnetic fluid layer bounded by two vertical, nonmagnetic plates of infinite extent. Two parallel plates, at x = ±d, and the Cartesian coordinates (x, y, z) subjected to a right-handed system, with its origin maintained in the centre between two plates, are considered in the problem. The x-axis is able to expand both positively and negatively and is perpendicular to the plates. The coordinate system is chosen such that the gravitational acceleration vector is expressed as (0, −g, 0), where g denotes the acceleration due to gravity. The plates are maintained at fixed temperatures $T_*\pm\Theta$. An external magnetic field of uniform magnitude is applied to the system at an inclination angle δ with respect to the x-axis. The field components are therefore given by $H_x^e = H^e \cos\delta$, $H_y^e = H^e \sin\delta\cos\gamma$, $H_z^e = H^e \sin\delta\sin\gamma$, where γ represents the azimuthal angle, defined as the angle between the y-axis and the projection of $H^e$ on the yz-plane. Within the fluid, the applied magnetic field $H^e$ induces an internal magnetic field H of magnitude *H*, which in turn produces a magnetization field M of magnitude *M*. The magnetization is assumed to be linearly proportional to the induced field and directed along it, such that $M = \chi_* H$, where $\chi_*$ denotes the fluid's effective (or integral) magnetic susceptibility. For analytical tractability, the temperature difference between the plates, Θ, is considered sufficiently small to justify the use of the Boussinesq approximation.

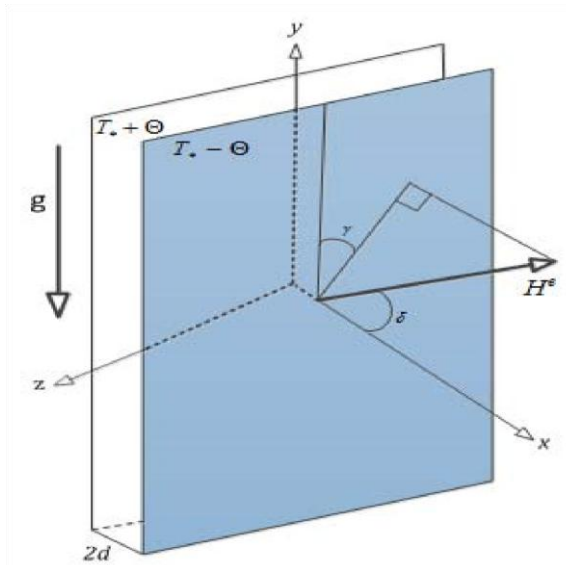


Fig. 2.1. Experimental model for problem geometry reported in our previous research work [12].

Consequently, this approximation is applied to the governing equations of continuity, momentum (Navier–Stokes), and energy. In addition, since ferrofluids have insignificant electrical conductivity, in the magneto-static form we incorporate the Maxwell equations of the magnetic field for the complements of these equations as described in [5]. The above-mentioned governing equations including velocity $\boldsymbol{v} = (u, v, w)$, the expressions for the magnetic field $H$, temperature $T$, magnetization $M$ and pressure $p$ are provided in Suslov and Rahman [11, 15] and are written as follows:

$$\nabla . \boldsymbol{v} = 0, \tag{2.1}$$

$$\rho_* \frac{\partial \boldsymbol{v}}{\partial T} + \rho_* \boldsymbol{v} . \nabla \boldsymbol{v} + \nabla p = \eta_* \nabla^2 \boldsymbol{v} + \rho \mathbf{g} + \mu_0 M \nabla H, \tag{2.2}$$

$$\frac{\partial T}{\partial t} + \boldsymbol{v} . \nabla T - \kappa_* \nabla^2 T = 0, \tag{2.3}$$

$$\nabla \times H = 0, \ \nabla . B = 0, \tag{2.4}$$

where,
$$B = \mu_0 (H + M), \ M = \frac{M\,(H,\ T)}{H} H, \tag{2.5}$$

$$\mu_0 \mathrm{M} \nabla H = \mu_0 [M_* + \chi \Delta H - K \Delta T] \nabla H = \mu_0 \nabla [M_* H + \frac{1}{2} \chi^2 \Delta H^2] - \mu_0 K \Delta T \nabla H, \tag{2.6}$$

$M_* = \chi_* H_*$, and $H_*$ are the magnitude of magnetization and magnetic field at the reference location with temperature $T_*$, $\chi_*$ is the integral magnetic susceptibility, $\chi = \partial M / \partial H |_{(H_*, T_*)}$ is the differential magnetic susceptibility, $K = -\partial M / \partial T |_{(H_*, T_*)}$ is the pyromagnetic coefficient, $t$ denotes time, $T$ the temperature, $p$ the pressure, $\boldsymbol{B}$ the magnetic flux density, and $\mu_0$ the magnetic permeability of free space. The magnetization characterises as linear when the magnetic susceptibilities $\chi$ and $\chi_*$ carry equal values, otherwise magnetization is nonlinear in the flow domain. The fluid properties at the reference temperature $T_*$ namely; density $\rho_*$, dynamic viscosity $\eta_*$, and thermal diffusivity $\kappa_*$ are indicated using the subscript $*$. Under the assumption of a small temperature difference between the hot and cold walls, the Boussinesq approximation is considered valid. Accordingly, the variation of fluid density is expressed as:

$$\rho = \rho_* [1 + \beta_* (T - T_*)], \tag{2.7}$$

where, $\beta_*$ denotes the thermal expansion coefficient evaluated at the reference temperature $T_*$. The MATLAB software is used to solve the equations and get the numerical results for this problem. Particularly, the

eigenvalue problem is revealed utilizing the MATLAB built-in function "eig". The Chebyshev expansion methods reported in [16] and [17] used for the numerical results of this problem. The previously presented equations transforming into the basic, and the linearized perturbation equations with the help of the generalized Squire's transformations are solved using numerical methods, and the computed numerical results are systematically analysed and depicted in Section 3.

## 3. Results and Discussion

### 3.1. Characteristics of Flow Stability in a Normal Field

The stability properties of a ferromagnetic fluid flow in a vertically heated layer situated in a normal magnetic field were investigated in Suslov's earlier study [11]. Flow stability in fluids that linearly magnetized with a particular Prandtl number of $\widetilde{Pr} = 130$ is the sole topic the author has discussed. Rahman and Suslov [15, 18] investigated the characteristics of the thermomagnetic convective flow of ferromagnetic fluid with a Prandtl number of $\widetilde{Pr} = 55$. Rahman et al. [19] analysed the mixed convective flow characteristics for the water-and kerosene- based fluids, whose Prandtl numbers $\widetilde{Pr}$ = 13.4 and 21 are considered, respectively, as presented by Khan et al. [20]. This current research addresses the whole stability properties of convective flow with linear and non-linear magnetization for the carrier liquid of ethylene glycol with Prandtl number, $\widetilde{Pr} = 40.36$ at room temperature (approximately 30°C) reported in [10], and various field inclination angles. In previous, many researchers have chosen water, kerosene, engine oil, protein solutions etc. as base liquids in their research works, but they did not compare the results with those used ethylene glycol as a base liquid. It is noticed that there is research gap, and thus we have considered ethylene glycol as a carrier liquid in the present research to analyse its characteristics and investigate its effects in a flow domain compared to the other carrier liquids. In this research, the convective flow characteristics to be investigated considering the critical values of $\widetilde{Gr}_{\mathrm{m}}$ as 5, 10 and 35 (see Table 3.1.1). For these considered values of $\widetilde{Gr}$ (say 5 or 10 or 35) and the rising values of $\widetilde{Gr}_{\mathrm{m}}$, it is found the wavenumber $\tilde{\alpha}$ grows in accordingly with the rising values of $\widetilde{Pr}$. On the other hand, for the fixed values of $\widetilde{Gr}_{\mathrm{m}}$ and the increasing values of $\widetilde{Gr}$ , it is noticed that the disturbance wave speed $\tilde{c}$, and the maximum basic flow velocity $\tilde{v}_{0max}$ gradually decreasing for the uprising values of $\widetilde{Pr}$. This study employed $\widetilde{Gr}$ as a metric with 5, 10 and 35 denoting the same trait mentioned in Rahman and Suslov [18]. While the Prandtl number $\widetilde{Pr}$ rises at arbitrarily fixed $\widetilde{Gr}_{\mathrm{m}}$ the critical value of $\widetilde{Gr}$ reduces and remains constant when $\widetilde{Gr} = 0$ or when there is no buoyancy force. Stated otherwise, the method provided a stationary magneto-convection starts at a wave number that does not depend on the values of $\widetilde{Pr}$ values when $\widetilde{Gr} = 0$. Furthermore, the data in Table 3.1.1 provides extra proof that the $\widetilde{Gr}$, which is reciprocally proportional to $\widetilde{Pr}$, characterizes the magneto-convection in stationary pattern. When the magnetic Grashof number $\widetilde{Gr}_m$ is larger, it indicates that magnetic (Lorentz) forces are stronger than viscous forces, which greatly affect fluid motion, reduce disturbances, and increase flow stability. Notably, the wave propagation disturbance in instability modes due to gravitational activity increases more quickly than that of the base flow velocity rising maximum in a flow domain with a high Prandtl number, suggesting that the physical properties of instabilities have no bearing on the basic flow velocity field. Furthermore, it is seen that the fundamental flow becomes more stable as the Prandtl number increases. A high Prandtl number denotes low thermal diffusion, since it is the product of fluid kinematic viscosity and inverse thermal diffusivity, that is, $\widetilde{Pr}$ = (viscous diffusion)/ (viscous diffusion) = $\mu/\kappa$.

Table 3.1.1: Critical values of $\widetilde{Gr}_{\mathrm{m}}$, $\widetilde{Gr}$, $\tilde{\alpha}$, speed of disturbance $\tilde{c}_c = -\tilde{\sigma}^{\mathrm{I}}/\tilde{\alpha}$, and maximum base flow velocity $\tilde{v}_{0max}$ at δ = 0°, $\mathrm{H}^{\mathrm{c}}$ = 100 and $\tilde{\chi} = 5 = \tilde{\chi}_*$ for different $\widetilde{P_r}$ values.

| $\widetilde{P_r}$ | $\widetilde{Gr}_{\mathrm{mc}}$ | $\widetilde{Gr}_{\mathrm{c}}$ | $\tilde{\alpha}_c$ | $\tilde{c}_c$ | $\tilde{v}_{0max}$ |
|---|---|---|---|---|---|
| 20 | 5 | 149.98 | 0.679 | ±9.232 | 9.616 |
| 27.5 | 5 | 106.48 | 0.874 | ±6.662 | 6.828 |
| 40.36 | 5 | 77.92 | 1.085 | ±4.950 | 5.327 |

| | | | | | |
|---|---|---|---|---|---|
| 55 | 5 | 62.97 | 1.153 | ±4.040 | 4.038 |
| 70 | 5 | 54.04 | 1.200 | ±3.489 | 3.465 |
| 130 | 5 | 37.10 | 1.308 | ±2.423 | 2.379 |
| 150 | 5 | 33.96 | 1.333 | ±2.222 | 2.178 |
| 20 | 10 | 149.08 | 0.828 | ±9.172 | 9.559 |
| 27.5 | 10 | 105.10 | 0.978 | ±6.568 | 6.739 |
| 40.36 | 10 | 75.91 | 1.103 | ±4.812 | 4.728 |
| 55 | 10 | 60.38 | 1.183 | ±3.862 | 3.872 |
| 70 | 10 | 50.93 | 1.241 | ±3.274 | 3.266 |
| 130 | 10 | 31.98 | 1.401 | ±2.070 | 2.051 |
| 150 | 10 | 28.06 | 1.447 | ±1.815 | 1.799 |
| 20 | 35 | 144.37 | 0.845 | ±8.855 | 9.257 |
| 27.5 | 35 | 97.39 | 1.025 | ±6.043 | 6.245 |
| 40.36 | 35 | 63.01 | 1.225 | ±3.930 | 3.567 |
| 55 | 35 | 38.29 | 1.459 | ±2.354 | 2.455 |
| 70 | 35 | 23.74 | 1.651 | ±1.395 | 1.523 |
| 130 | 35 | 11.03 | 1.498 | ±0.535 | 0.708 |
| 150 | 35 | 7.07 | 1.234 | ±0.269 | 0.453 |

Table 3.1.2: Critical values of $\widetilde{Gr}_m$ , $\widetilde{Gr}_c$, $\tilde{\alpha}_c$, speed of disturbance $\tilde{c}_c = -\tilde{\sigma}^I/\tilde{\alpha}$, for leading two waves of mixed convection at (δ = 0°), $H^e$ = 100, $\widetilde{Gr}_m$=15, $\widetilde{Pr}$=40.36 and different $\tilde{\chi}$ and $\tilde{\chi}_*$ values.

| | | Upward Propagation wave | | | Downward Propagation wave | | |
|---|---|---|---|---|---|---|---|
| $\tilde{\chi}$ | $\tilde{\chi}_*$ | $\tilde{\alpha}_c$ | $\widetilde{Gr}_c$ | $\tilde{c}_c$ | $\tilde{\alpha}_c$ | $\widetilde{Gr}_c$ | $\tilde{c}_c$ |
| 5 | 5 | 1.123 | 73.75 | 4.664 | 1.123 | 73.75 | -4.664 |
| 3 | 5 | 1.125 | 74.37 | 4.697 | 1.120 | 75.26 | -4.756 |
| 3 | 3 | 1.125 | 73.30 | 4.634 | 1.125 | 73.30 | -4.634 |
| 1.5 | 2.5 | 1.131 | 72.74 | 4.592 | 1.126 | 73.52 | -4.644 |
| 1 | 2 | 1.130 | 72.98 | 4.606 | 1.123 | 74.23 | -4.688 |
| 0.5 | 1.5 | 1.123 | 74.48 | 4.699 | 1.111 | 76.97 | -4.861 |
| 5 | 6 | 1.126 | 73.41 | 4.640 | 1.125 | 73.55 | -4.650 |
| 6 | 6 | 1.122 | 73.89 | 4.674 | 1.122 | 73.89 | -4.674 |
| 6.5 | 7.5 | 1.125 | 73.63 | 4.655 | 1.124 | 73.72 | -4.661 |
| 7 | 8.5 | 1.125 | 73.68 | 4.658 | 1.124 | 73.81 | -4.667 |
| 7 | 9 | 1.126 | 73.77 | 4.663 | 1.124 | 73.97 | -4.676 |
| 8 | 10 | 1.125 | 73.82 | 4.666 | 1.124 | 73.97 | -4.676 |
| 8 | 9.5 | 1.125 | 73.76 | 4.664 | 1.124 | 73.87 | -4.671 |
| 6 | 10 | 1.112 | 76.10 | 4.809 | 1.114 | 76.89 | -4.860 |
| 6 | 8 | 1.126 | 73.75 | 4.661 | 1.124 | 74.00 | -4.678 |

Therefore, thermal disturbances dissipate slowly in fluids with large Prandtl numbers. Consequently, from the information in Table 3.1.1, the basic flow attains more stability in the large Prandtl number of fluids as well as the uprising values of $\widetilde{Gr}_m$ . However, from the data in Table 3.1.1 it is concluded that the magnetically more dominated fluid flow becomes comparatively more stable, and the heat dominated flow gets less stable regardless of any Prandtl number of fluids. The instabilities discovered for $\widetilde{Gr}_m = 0$ have a physical cause that is dominated by heat. Gershuni and his associates called these types of waves are thermal waves [21].

The heated wall prompts the thermal waves to rise upward, and the cool wall drives them to move downward. Table 3.1.2 presents the critical values of the thermal Grashof number $\widetilde{Gr}_c$, wave number $\tilde{\alpha}_c$, and disturbance wave speed $\tilde{c}$ for both upward and downward propagating waves in the presence of a normal magnetic field ($\delta = 0^o$). The analysis is conducted under fixed parameters: $\widetilde{Gr}_m = 15, H^e = 100,$ and $\widetilde{Pr} = 40.36$, across various values of $\tilde{\chi}$ and $\tilde{\chi}_*$. The disturbance wave speed $\tilde{c}$ is behaving as positive for propagating waves in the upward direction and negative in the opposite direction, with magnitudes ranging approximately from 4.592 to 4.861. This indicates that while the direction of wave propagation differs, the absolute speed remains nearly symmetric, implying balanced dynamic behaviour in both directions. The critical Grashof number $\widetilde{Gr}_c$ varies moderately between 72.74 and 76.97, showing sensitivity to the values of $\tilde{\chi}$ and $\tilde{\chi}_*$. Meanwhile, the wave number $\tilde{\alpha}_c$ stays within a relatively narrow band between 1.111 and 1.131 suggesting that the most unstable wavelength is nearly constant throughout the examined parameter space. Notably, the downward propagating waves tend to exhibit slightly higher critical Grashof numbers and more negative wave speeds, reflecting the stronger damping effect of the normal field in the upward direction. This observation highlights the stabilizing influence of the magnetic field, especially on the upward convective modes. These results are essential for understanding the behavior of mixed convection flows in magnetohydrodynamic (MHD) systems and provide insight into the stability characteristics under magnetic influence, which are relevant in both engineering and geophysical contexts.

### 3.2. Characteristics of Flow Stability in an Oblique Field

The flow stability characteristics and comparison among them under the effects of inclined magnetic field for a few particular inclination angles will be investigated in this section.

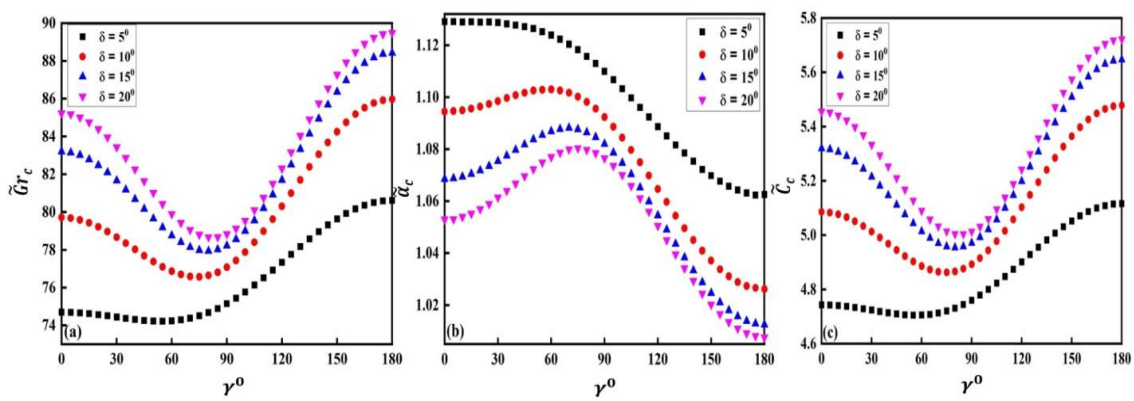


Fig. 3.2.1. Comparison among the critical parameter values: (a) Grashof number $\widetilde{Gr}_c$ (the flow is stable under the respective curves), (b) wave number $\tilde{\alpha}$ and (c) wave speeds $\tilde{c}_c$ as functions of the magnetic field orientation angle $\gamma$ for various field inclination angle $\delta$ at $\widetilde{Gr}_m$= 15, $H^e$ = 100, $\widetilde{\mathrm{Pr}}$= 40.36 and $\tilde{\chi} = \tilde{\chi}_* = 3$.

The Fig. 3.2.1 shows how three critical parameters $\widetilde{Gr}_c$, $\tilde{\alpha}_c$, and $\tilde{c}_c$, change with the magnetic field orientation or azimuthal angle $\gamma$ and field inclination angle $\delta$ at parameters values $\widetilde{Gr}_c$= 15, $H^e$ = 100, $\widetilde{Pr}$= 40.36, and $\tilde{\chi}$ = 3 = $\tilde{\chi}_*$. The Fig. 3.2.1(a) demonstrates that the thermal effect as $\widetilde{Gr}_c$, initially declines with rising $\gamma$, hitting a minimum near $\gamma$ = 75° and then progressively rises towards $\gamma$ = 180°. This tendency is consistent across all inclination angle values $\delta$. Furthermore, higher values of $\delta$ correspond to generally higher values of $\widetilde{Gr}_c$, showing enhanced flow instability with larger field inclination angles. The Fig. 3.2.1(b) depicts the critical wave number $\tilde{\alpha}_c$, which displays a minor increase in the interval $\gamma\approx$ 60° to 75° at larger field inclination angles, followed by a progressive drop. As $\delta$ grows, the curve moves downhill, indicating it has shorter wave numbers that is longer wavelengths, and result the most unstable modes occur at rising field inclination angles. The critical wave speed $\tilde{c}_c$ is shown in Fig.3.2.1(c). The wave speed shows a brief minimum close to $\gamma$ = 75° for all $\delta$, and then rises. For the situation of linear magnetization, which is defined by equal values of

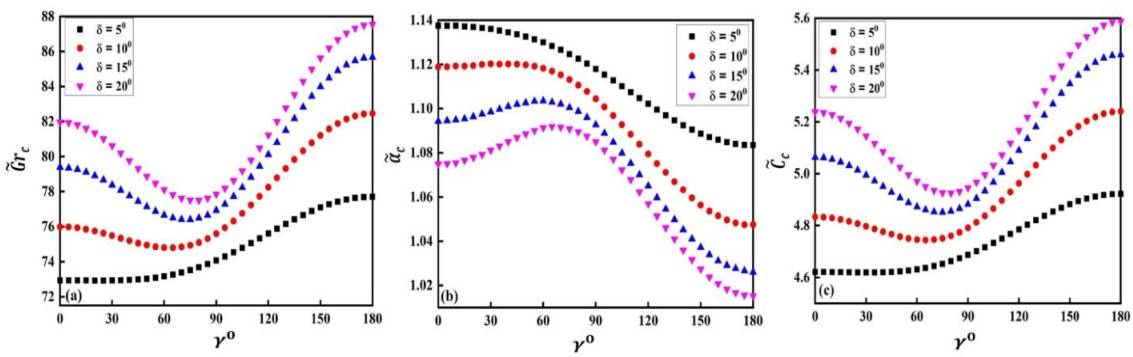


Fig. 3.2.2. Comparison among the critical parameter values: (a) Grashof number $\widetilde{Gr}_c$ (the flow is stable under the respective curves), (b) wave number $\tilde{\alpha}$ and (c) wave speeds $\tilde{c}_c$ as functions of the magnetic field orientation angle $\gamma$ for various field inclination angle $\delta$ at $\widetilde{Gr}_m$= 15, $H^e$ = 100, $\widetilde{\mathrm{Pr}}$ = 40.36 and $\tilde{\chi}$ = $\tilde{\chi}_*$= 5.

$\tilde{\chi}$ and $\tilde{\chi}_*$is 5, the magnitude of $\tilde{c}_c$ increases as $\delta$ increases, indicating that wave propagation is more noticeable under bigger inclined magnetic fields. Figure 3.2.2 provides a comparative illustration of the variation of three critical parameters; namely the critical values of $\widetilde{Gr}_c$ , the critical wave number $\tilde{\alpha}_c$, and the critical wave speed $\tilde{c}_c$ as functions of the field orientation angle $\gamma$, for various values of $\delta$, under fixed conditions: $\widetilde{Gr}_c$= 15, $H^e$ = 100, $\widetilde{Pr}$ = 40.36, and a linear magnetization model with $\tilde{\chi}$ = 5 = $\tilde{\chi}_*$. In Fig. 3.2.2(a), the critical value of $\widetilde{Gr}_c$ initially dropping with rising $\gamma$, hitting a minimum at close to $\gamma$ = 75°, and subsequently rises monotonically as $\gamma$ approaches to 180°. This non-monotonic trend is consistent across all considered values of $\delta$, and it is noticed that larger values of $\delta$ lead the higher values of $\widetilde{Gr}_c$, indicating enhanced flow instability in the larger field inclination angles. The Fig. 3.2.2(b) displays the behaviour of the critical wave number $\tilde{\alpha}_c$ which shows a mild rising up to approximately $\gamma$= 70° to 85°, followed by a continual decline. As the magnetic inclination angle $\delta$ increases, the corresponding $\tilde{\alpha}_c$ curves shift downward, suggesting that higher magnetic inclinations are associated with longer wavelength disturbances, thus modifying the nature of the most unstable convective modes. The Fig. 3.2.2(c) illustrates the variation of the critical wave speed $\tilde{c}_c$ with respect to $\gamma$. For all values of $\delta$ and $\tilde{c}_c$ reaches a minimal point near $\gamma$= 77.5° and rises thereafter. The wave speed $\tilde{c}_c$ rises progressively according to the rising value of $\delta$, which implies that wave interruption is more pronounced with larger magnetic field inclinations.

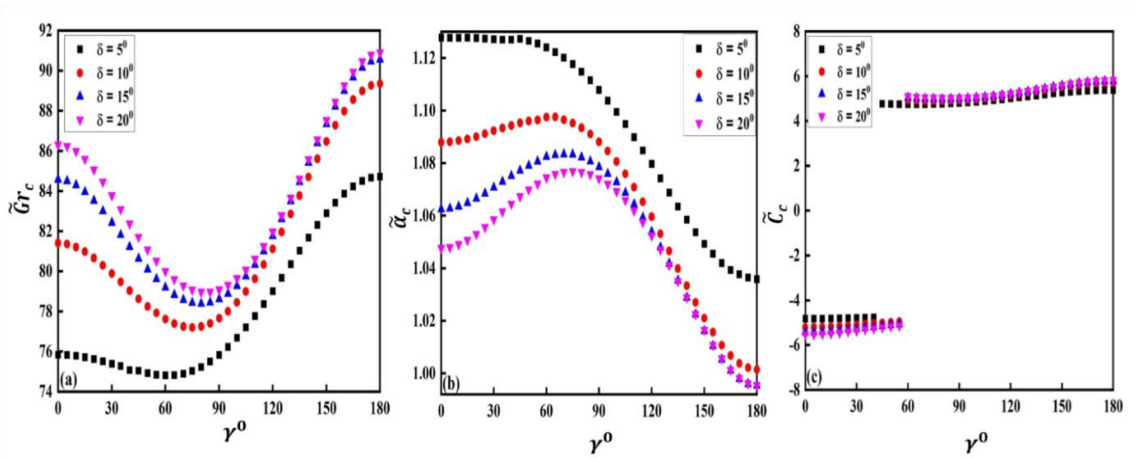


Fig. 3.2.3. Comparison among the critical parameter values: (a) Grashof number $\widetilde{Gr}_c$ (the flow is stable under the respective curves), (b) wave number $\tilde{\alpha}$ and (c) wave speeds $\tilde{c}_c$ as functions of the magnetic field orientation angle $\gamma$ for various field inclination angle $\delta$ at $\widetilde{Gr}_m$= 15, $H^e$ = 100, $\widetilde{\mathrm{Pr}}$ = 40.36, $\tilde{\chi}$ = 3 and $\tilde{\chi}_*$ = 5.

This highlights the significant role of magnetic anisotropy in influencing wave dynamics in the context of linear magnetization characterized by $\tilde{\chi} = \tilde{\chi}_* = 3$. The Fig. 3.2.3 demonstrate the characteristics of critical flow parameters depending on field orientation angle $\gamma$, for different values of the oblique angle $\delta$, at $\widetilde{Gr}_c$= 15, $H^e$ = 100, $\widetilde{\mathrm{Pr}}$ = 40.36, $\tilde{\chi}$ = 3, and $\tilde{\chi}_*$= 5. The Fig. 3.2.3(a) depicts the effects of $\widetilde{Gr}_c$, which defines the instability characters in fluid flow. The flow indicates stable underneath the continual curves in plot (a) in this figure. The values of $\widetilde{Gr}_c$ initially declines with rising $\gamma$ to all $\delta$, reaches to a minimal point close to $\gamma$ = 80º, and then upraises. This trend indicates the sensitivity most in flow stabilization with regard to field intermediate orientation angles. Furthermore, larger values of $\delta$ lead to increase $\widetilde{Gr}_c$, suggesting enhanced stabilization due to larger field inclination angles. The Fig. 3.2.3(b) presents the characteristics of the critical wave number $\tilde{\alpha}_c$. In beginning $\tilde{\alpha}_c$ upraises slightly at first, peaks between $\gamma$ = 60º and 90º to all $\delta$, and then gradual drops. This characteristic demonstrates the convective rolls with shorter wavelength be in control of intermediate angles, while longer wavelengths promote with higher values of $\gamma$. The Fig. 3.2.3(c) displays the critical wave speed $\tilde{c}_c$. It remains nearly constant and negative across the range $\gamma$ = 0º to approximately 60º and then transitions to positive values, maintaining a nearly constant trend thereafter. This implies that inclination angles have minimal effect on wave propagation speed. The negative values of $\tilde{c}_c$at lower $\gamma$ suggest the presence of backward-moving or damped waves, indicating the existence of propagating wave modes associated with nonlinear magnetization, as characterized by the unequal values of $\tilde{\chi}$ = 3 and $\tilde{\chi}_*$= 5. Collectively, these trends conclude that the critical influence of both $\gamma$ and $\delta$ on the threshold of magneto-convection. Increasing the magnetic inclination angle enhances flow instability, shifts the dominant wave numbers toward longer wavelengths, and intensifies the propagation speed of instabilities, thus playing a decisive role in the system overall dynamic behaviour in the flow domain.

### 3.3. Comparison of Flow Stabilization under Stronger and Weaker Magnetic Field Effects

A detailed comparison between the weaker ($H^e$ = 10) and stronger ($H^e$ = 1000) magnetic field cases reveals the significant influence of magnetic field intensity on the critical parameters governing the onset of double diffusive convection.

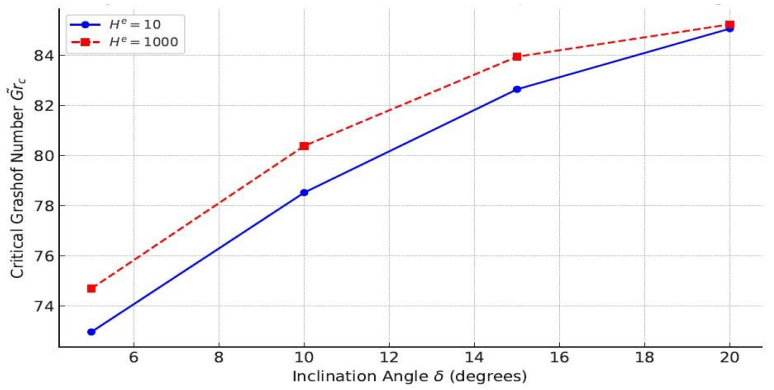


Fig. 3.3.1. Comparison of flow stabilization represented by critical thermal Grashof number $\widetilde{Gr}_c$ as a function of field inclination angle $\delta$ at ($\delta$ = 5º, 10º, 15º, 20º) for $\gamma$ = 0º, $\tilde{\chi} = \tilde{\chi}_* = 5$, $\widetilde{Pr}$ = 40.36 and magnetic field strengths $H^e$ = 10 and $H^e$ = 1000.

From the Fig. 3.3.1, it is evident that the critical Grashof number $\widetilde{Gr}_c$ increases with the application of the stronger magnetic field compared to the weaker magnetic field effects for all arbitrarily chosen magnetic field inclination angles ($\delta$ = 5º, 10º, 15º and 20º), and any combinations $\tilde{\chi}$ and $\tilde{\chi}_*$. As follows the Fig. 3.3.1, particularly when $\tilde{\chi} = \tilde{\chi}_* = 5$, $\widetilde{Gr}_c$ increases from 72.96 to 74.69 at $\delta$ = 5º, from 79.08 to 79.71 at $\delta$ = 10º, from 82.85 to 83.17 at $\delta$ = 15º, and from 85.06 to 85.23 at $\delta$ = 20º, respectively for $H^e$ = 10 and $H^e$ = 1000. These increases in $\widetilde{Gr}_c$ clearly indicate a flow destabilization due to the inclined magnetic field effect. It is clear that obliquely applied stronger magnetic field suppresses less the flow disturbances compared to the weaker magnetic field though they introduce the Lorentz forces that resist convective instabilities. As a result, a stronger thermal gradient is required to initiate convection when the applied inclined magnetic field is weaker intensified.

**3.4. Effects of Prandtl Number and Field Inclination on Flow Stabilization**

A detailed investigation has been performed to evaluate the influence of the Prandtl number $\widetilde{Pr}$ on the linear stability behavior of thermally driven magnetohydrodynamic (MHD) flows. The analysis is carried out for two representative cases of the critical Grashof number, $\widetilde{Gr}_c$ = 15 and $\widetilde{Gr}_c$ = 12, under the effect of externally imposed magnetic fields with intensities $H^e$ = 10 and $H^e$ = 100. To incorporate directional magnetic effects, three inclination angles are considered: $\delta$ = 0º, 5º and 10º. For each combination of $\widetilde{Gr}_c$ , $H^e$, and $\delta$, five fixed values of the Prandtl number $\widetilde{Pr}$ = 130, 55, 40.36, 27.5, and 21 are examined, covering a broad physical range from low thermal diffusivity (high $\widetilde{Pr}$) to high thermal diffusivity (low $\widetilde{Pr}$). The results reveal that variations in $\widetilde{Pr}$ significantly influence the growth rate and stability characteristics of the flow. Higher Prandtl numbers tend to enhance the stabilizing effects of the magnetic field, delaying the onset of instability, whereas lower $\widetilde{Pr}$ values promote thermal diffusion and shift the instability thresholds accordingly. This comparative analysis elucidates the critical role of thermal transport properties in conjunction with magnetic and buoyant forces, providing important insight into the physical mechanisms driving MHD boundary layer stability. The Fig. 3.4.1 presents the variation of the temporal amplification rates $\tilde{\sigma}^R$(left graph) and the corresponding frequencies $\tilde{\sigma}^I$(right plot) as functions of the resultant wavenumber $\tilde{\alpha}$, for various Prandtl numbers ($\widetilde{Pr}$ = 130, 55, 40.36, 27.5, 21) under conditions $\delta = \gamma$ = 0º, $H^e$ = 10, $\tilde{\chi} = \tilde{\chi}_* = 5$, $\widetilde{Gr}$ = 0 and $\widetilde{Gr}_m$ = 15. In the left plot, $\tilde{\sigma}^R$ initially increases with $\tilde{\alpha}$, reaches a maximum, and then decreases, thus forming a stability envelope corresponding to each Prandtl number. Higher values of $\widetilde{Pr}$ result in greater peak growth rates, indicating that thermal diffusivity plays a substantial role in influencing the system's instability.

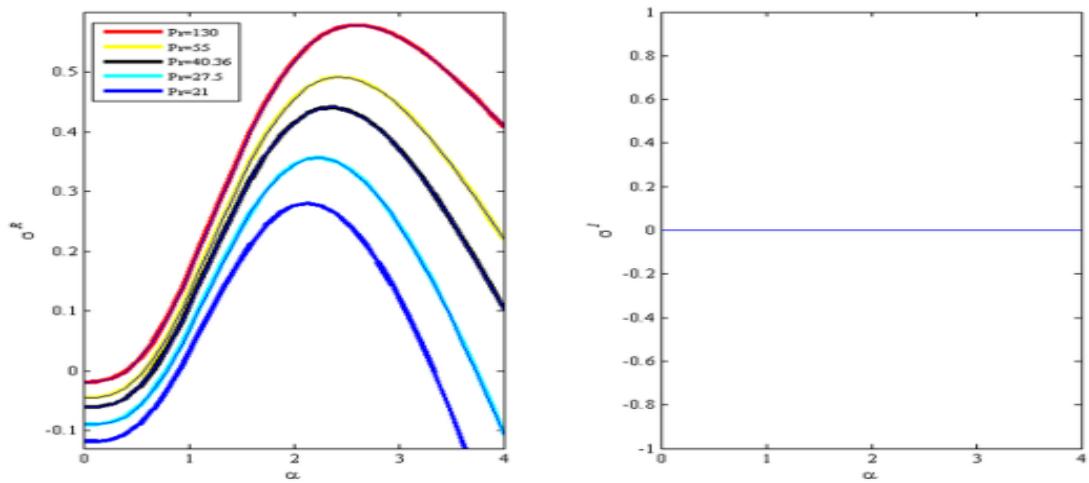


Fig. 3.4.1. Variation of the temporal amplification rates $\tilde{\sigma}^R$(left) and frequencies $\tilde{\sigma}^I$(right) as functions of the resultant wavenumber $\tilde{\alpha}$ at $\gamma = 0^o$, $(\widetilde{Gr}_m, \widetilde{Gr}) = (15, 0)$, $H^e = 10$ and $\delta = 0^o$.

The occurrence of positive values of $\tilde{\sigma}^R$over a finite range of $\tilde{\alpha}$ confirms the presence of temporally growing modes, signifying that the flow is unstable within those wavenumber intervals. In contrast, the right plot in Fig. 3.4.1 demonstrates that the frequency $\tilde{\sigma}^I$ remains identically zero across all values of $\tilde{\alpha}$, implying that the instability is purely stationary in nature. There is no oscillatory component, and perturbations amplify without any phase propagation. For the present case of aligned magnetic fields ($\delta = \gamma = 0^o$), this result reinforces the conclusion that the system exhibits non-oscillatory (stationary) instabilities, whose growth dynamics are strongly modulated by the Prandtl number. These findings conclude the critical role of thermal and viscous diffusion mechanisms in determining the onset and character of magneto-thermal convection. The Fig. 3.4.2 illustrates the influence of Prandtl number on the temporal growth rates $\tilde{\sigma}^R$(left) and oscillation frequencies $\tilde{\sigma}^I$(right) as functions of the resultant wavenumber $\tilde{\alpha}$, for a set of parameters values same as parameters used in Fig. 3.4.1 but magnetic inclination angle $\delta = 5^o$. In the left plot in Fig. 3.4.2 the amplification rate curves show a characteristic peak for each Prandtl number, again indicating the presence of instability over a range of wave numbers. As in the previous figure, higher Prandtl numbers lead to higher peak growth rates, suggesting the qualitatively similar but quantitatively less instability in fluids with lower temporal amplification rate under the effect of magnetic field for smaller field inclination angle. The right plot, showing $\tilde{\sigma}^I$, now displays small but nonzero negative values across the spectrum of $\tilde{\alpha}$, implying the emergence of weakly damped oscillations. This is a departure from the purely stationary modes observed in the zero-inclination case (see Fig. 3.4.1), and indicates that even a slight magnetic field inclination $\delta = 5^o$ introduces a minor travelling-wave component to the instability. This result is significant as it shows that the inclination of the magnetic field, even if small, can qualitatively change the nature of the instability from stationary to weakly oscillatory, adding a layer of complexity to the flow behaviour and its control. The Fig. 3.4.3 shows how the Prandtl number effects on the temporal growth rates $\tilde{\sigma}^R$(left) and oscillation frequencies $\tilde{\sigma}^I$(right) as functions of the resultant wavenumber $\tilde{\alpha}$ and parameters values same as in Fig. 3.4.1 but $\delta = 10^o$. As seen in Fig. 3.4.3 the left plot represents temporal amplification rate in qualitatively similar but quantitatively a small deviate compared to the previous one.

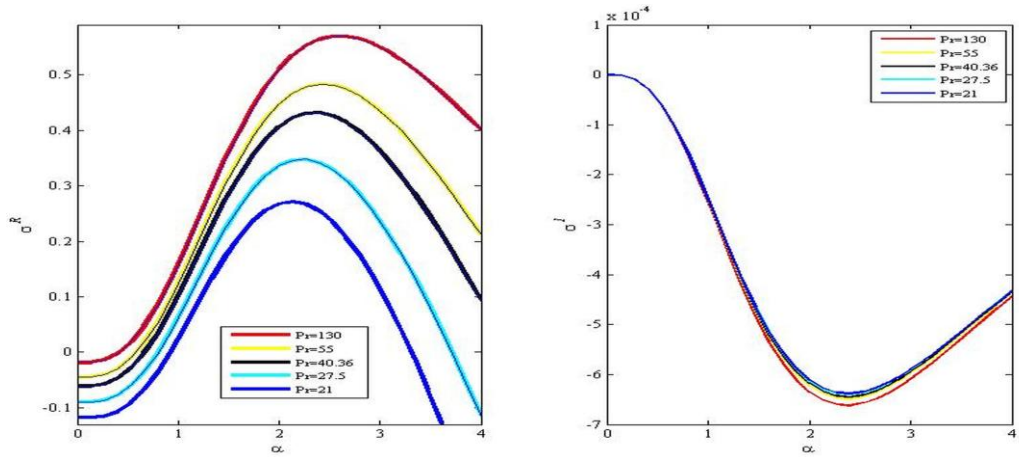


Fig. 3.4.2. Variation of the temporal amplification rates $\tilde{\sigma}^R$(left) and frequencies $\tilde{\sigma}^I$(right) as functions of the resultant wavenumber $\tilde{\alpha}$ at $\gamma = 0^o$, $(\widetilde{Gr}_m, \widetilde{Gr}) = (15, 0)$, $H^e = 10$ and $\delta = 5^o$.

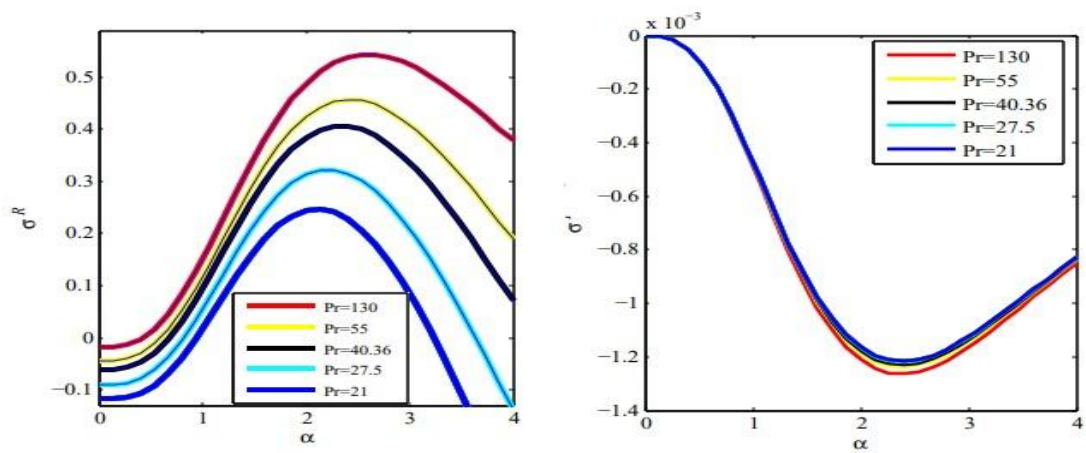


Fig. 3.4.3. Variation of the temporal amplification rates $\tilde{\sigma}^R$(left) and frequencies $\tilde{\sigma}^I$(right) as functions of the resultant wavenumber $\tilde{\alpha}$ at $\gamma = 0^o$, $(\widetilde{Gr}_m, \widetilde{Gr}) = (15, 0)$, $H^e = 10$ and $\delta = 10^o$.

With the increasing field inclination angle enhancing the comparatively a little bit more stabilization in temporal amplification (see in the left plot in Fig. 3.4.3). The temporal frequency shown in the right plot in Fig. 3.4.3 which is amplified by the effect of larger inclined magnetic field. Overall, the results show that when the field inclination angle increases, the temporal amplification marginally decreases while the corresponding frequency increases significantly and the system experiences oscillatory instability.

## 4. Conclusions

The linear stability of thermomagnetic convection in the ethylene glycol based magnetic fluid layer enclosed by two differentially heated vertical walls is investigated comprehensively. The impacts of

thermogravitational buoyancy and magnetic forces due to the effects of temperature variance, field orientation angle and intensity of magnetic field that play the critical roles in flow stabilization in the flow domain. Consequently, the following conclusions can be made in light of the findings and discussions:
The basic flow attains more stability in the large Prandtl number of fluids as well as the stronger magnetic sensitive fluids in normal applied magnetic field to the walls. In the normal magnetic field case, the upward propagating waves becomes slightly more stable compared to the downward propagating waves due to gravitational action on the convective modes. The magnetically more dominated fluid flow becomes comparatively more stable, and the heat dominated flow gets less stable with regardless of any Prandtl number of fluids under perpendicular magnetic field effects. The stronger inclined magnetic field consistently corresponds to more basic flow instable configuration compared to the weaker inclined magnetic field case. The dominant destabilizing effect of the magnetic field is mechanical, rather than thermal or solutal (the dissolved material) in the flow domain. The wave number becomes smaller indicating the longer wavelengths, the wave propagation is more pronounced, and finally the fluid flow becomes more instable under larger inclined magnetic field effects with regardless of the fluid magnetization is linear or not.

**Acknowledgements**
All authors contributed to the study conception and design. Material preparation, data curation and analysis were performed by Md. Habibur Rahman and Sushmita Mondal. The first draft of this manuscript was written by Sushmita Mondal and Md. Habibur Rahman performed writing-review and editing and supervision. All authors read, commented and approved the final manuscript.

**Funding**
The authors declare that no funds, grants, or other support were received during the preparation of this manuscript.

**References**
[1] Odenbach, S. (2002). Ferrofluids: Magnetically controllable fluids and their applications. Springer.
[2] Elmore, W. C. (1938). The magnetisation of ferromagnetic colloids. Physical Review, 54, 1092–1095.
[3] Bashtovoy, V. G., Berkovsky, B. M., & Vislovich, A. N. (1988). Introduction to thermomechanics of magnetic fluids. Hemisphere.
[4] Rosensweig, R. E. (1979). Fluid dynamics and science of magnetic fluids. Advances in Electronics and Electron Physics, 48, 103–199.
[5] Rosensweig, R. E. (1985). Ferrohydrodynamics. Cambridge University Press.
[6] Blums, E. Ya., Maiorov, M. M., & Tsebers, A. O. (1989). Magnetic fluids. Zinatne. (in Russian)
[7] Blums, E., Tsebers, A. O., & Maiorov, M. M. (1997). Magnetic fluids. Walter de Gruyter.
[8] Nakatsuka, K., Hama, Y., & Takahashi, J. (1990). Heat transfer in temperature-sensitive magnetic fluid. Journal of Magnetism and Magnetic Materials, 85, 207–209.
[9] Tynjälä, T. (2005). Theoretical and numerical study of thermomagnetic convection in magnetic fluids (Doctoral dissertation, Lappeenranta University of Technology).
[10] Minhas, H., & Lock, G. S. H. (1996). Estimating the influence of Prandtl number on heat transfer in a bayonet tube. International Communications in Heat and Mass Transfer, 23(7), 1011–1017.
[11] Suslov, S. A. (2008). Thermo-magnetic convection in a vertical layer of ferromagnetic fluid. Physics of Fluids, 20(8), 084101.
[12] Mohammad, A. T., Sadia, S., Kamrujjaman, M., & Mamun, M. M. (2022). Free convection of temperature-dependent thermal conductivity based ethylene glycol–Al2O3 nanofluid in an open cavity with wall heat flux. International Communications in Heat and Mass Transfer, 138, 106379.

[13] Farhad, H. M., Mamun, M. M., Kamrujjaman, M., & Sadia, S. (2022). Natural convection flow over a vertical permeable circular cone with uniform surface heat flux in temperature-dependent viscosity with three-fold solutions within the boundary layer. Computation, 10(4), 60.
[14] Rahman, H. (2024). Investigation of thermomagnetic gravitational convection and energy distribution in a vertical layer of ferrofluid. Journal of Thermal Engineering, 10(4), 936–953.
[15] Rahman, H., & Suslov, S. A. (2015). Thermomagnetic convection in a layer of ferrofluid placed in a uniform oblique external magnetic field. Journal of Fluid Mechanics, 764, 316–348.
[16] Ku, H. C., & Hatziavramidis, D. (1984). Chebyshev expansion methods for the solution of the extended Graetz problem. Journal of Computational Physics, 56, 495–512.
[17] Hatziavramidis, D., & Ku, H. C. (1985). An integral Chebyshev expansion method for boundary-value problems of ODE type. Computers & Mathematics with Applications, 11(6), 581–586.
[18] Rahman, H., & Suslov, S. A. (2016). Magneto-gravitational convection in a vertical layer of ferrofluid in a uniform oblique magnetic field. Journal of Fluid Mechanics, 795, 847–875.
[19] Rahman, H., Hossen, R. R., Mondal, S., & Hasibur, H. (2024). Investigation of thermomagnetic convective flow in vertical layers between water and kerosene-based magnetic fluids. Journal of Umm Al-Qura University for Applied Sciences, 10, 457–473.
[20] Khan, W. A., Khan, Z. H., & Haq, R. U. (2015). Flow and heat transfer of ferrofluids over a flat plate with uniform heat flux. European Physical Journal Plus, 130, 86–98.
[21] Gershuni, G. Z., Zhukhovitsky, E. M., & Nepomniaschy, A. A. (1989). Stability of convective flows. Science. (in Russian)